

Title: SEC23B is required for pancreatic acinar cell function in adult mice.

Running title: SEC23B deletion in acinar cells

Rami Khoriaty^a, Nancy Vogel^{b*}, Mark J. Hoenerhoff^c, M. Dolores Sans^b, Guojing Zhu^d, Lesley Everett^{e†}, Bradley Nelson^b, Haritha Durairaj^b, Brooke McKnight^{†‡}, Bin Zhang^g, Stephen A. Ernst^h, David Ginsburg^{a,d,i,j||}, John A. Williams^{a,b||}

^aDepartment of Internal Medicine, University of Michigan, Ann Arbor, MI;

^bDepartment of Molecular and Integrative Physiology, University of Michigan, Ann Arbor, MI;

^cIn Vivo Animal Core, Unit for Laboratory Animal Medicine, University of Michigan, Ann Arbor, MI;

^dLife Sciences Institute, University of Michigan, Ann Arbor, MI;

^eUniversity of Michigan Medical School, Ann Arbor, MI;

^fCollege of Literature Science and the Arts, University of Michigan, Ann Arbor, MI;

^gGenomic Medicine Institute, Cleveland Clinic Lerner Research Institute, Cleveland, OH;

^hDepartment of Cell and Developmental Biology, University of Michigan, Ann Arbor, MI

ⁱDepartments of Human Genetics and Pediatrics and Communicable Diseases, University of Michigan, Ann Arbor, MI;

^jHoward Hughes Medical Institute, University of Michigan, Ann Arbor, MI

*Current address: Department of Biology, Eastern Michigan University, Ypsilanti, MI

†Current address: Department of Ophthalmology, University of California San Francisco, San Francisco, CA

‡Current address: Department of Oncology, Wayne State University School of Medicine, Detroit, MI

|| Corresponding authors:

John A. Williams

Email: jawillms@med.umich.edu

Phone:(734) 647-2886

Fax: (734) 936-8813

and

David Ginsburg

Email: ginsburg@umich.edu

Phone: 734-647-4808

Fax: 734-936-2888

Abstract

Mice with germline absence of SEC23B die perinatally, exhibiting massive pancreatic degeneration. We generated mice with tamoxifen-inducible, pancreatic acinar cell-specific *Sec23b* deletion. Inactivation of *Sec23b* exclusively in the pancreatic acinar cells of adult mice results in decreased overall pancreatic weights from pancreatic cell loss (decreased pancreatic DNA, RNA, and total protein content), as well as degeneration of exocrine cells, decreased zymogen granules, and alterations in the endoplasmic reticulum (ER), ranging from vesicular ER to markedly expanded cisternae with accumulation of moderate density content or intracisternal granules. Acinar *Sec23b* deletion results in induction of ER stress and increased apoptosis in the pancreas, potentially explaining the loss of pancreatic cells and decreased pancreatic weight. These findings demonstrate that SEC23B is required for normal function of pancreatic acinar cells in adult mice.

Introduction

SEC23 is a core component of coat protein complex II (COPII) vesicles, which transport secretory proteins from the endoplasmic reticulum (ER) to the Golgi apparatus. The genes encoding COPII vesicle components are highly evolutionarily conserved; however, in contrast to yeast, the mammalian genome contains two or more paralogs for most of these genes (Bonifacino and Glick, 2004; Khoriaty et al., 2012; Zanetti et al., 2012). The two mammalian paralogs for SEC23, SEC23A and SEC23B, exhibit ~85% amino acid sequence identity (Bonifacino and Glick, 2004; Khoriaty et al., 2012; Zanetti et al., 2012). In humans, *SEC23A* mutations result in cranio-lenticulo-sutural dysplasia, an autosomal recessive disease characterized by late closure of fontanelles, skeletal abnormalities, and sutural cataracts (Boyadjiev et al.; Lang et al., 2006), while homozygous/compound heterozygous loss of function *SEC23B* mutations result in congenital dyserythropoietic anemia type II (CDAlI) (Bianchi et al., 2009; Khoriaty et al., 2012; Schwarz et al., 2009), a disease characterized by a defect in erythroid maturation. We previously reported that mice genetically deficient for *SEC23A* exhibit mid-embryonic lethality and a cranial developmental defect (Zhu et al., 2015), while mice homozygous for a *Sec23b* null allele die perinatally with massive pancreatic degeneration (Tao et al., 2012). Mice with embryonic pancreas-specific SEC23B deficiency recapitulated the latter phenotype (Khoriaty et al., 2016), with pancreas tissues harvested from these mice demonstrating abnormal acinar cell histology, but normal appearing islet cells.

The pancreas is a professional secretory organ with two highly active cell types engaged in protein synthesis and secretion, the exocrine acinar cell, which secretes digestive enzymes, and the endocrine beta and alpha cells, which secrete insulin and glucagon, respectively. Acinar cells contain abundant rough endoplasmic reticulum (RER), prominent Golgi, and large secretory granules termed zymogen granules (ZG) (Gorelick and Jamieson, 2012). About 20 different digestive enzymes are synthesized on the RER and traverse the

secretory pathway, with the ER to Golgi being a major concentrating step (Oprins et al., 2001). The early steps by which coated vesicles bud from smooth regions of the ER termed transition zones appear similar in acinar cells compared to other secretory cells. The concentrations of amylase and chymotrypsinogen are similar in the COPII vesicle and the RER lumen, suggesting a bulk flow process for this initial step (Barlowe and Helenius, 2016; Klumperman, 2000; Martinez-Menarguez et al., 1999).

To test whether SEC23B is required for normal pancreatic function in adult mice, we now report the characterization of mice with tamoxifen-inducible, acinar cell-specific SEC23B deficiency. Tamoxifen administration to adult mice results in loss of pancreatic mass with evidence of cell loss, degeneration of exocrine cells (with smaller than normal zymogen granules and ER dilation), ER stress, and increased pancreatic cell apoptosis.

Results

Generation of mice with tamoxifen-inducible pancreatic acinar cell specific *Sec23b* deletion

Mice with tamoxifen-inducible acinar cell specific deletion of *Sec23b* were generated by crossing *Sec23b*^{+/-} CreErT⁺ mice to *Sec23b*^{fl/fl} mice. This cross yielded the expected number of *Sec23b*^{fl/fl} CreErT⁺ mice at weaning (Table 1). One week post tamoxifen administration, pancreas tissues were harvested from the latter mice to determine the degree of excision of *Sec23b*. *Sec23b*^{fl/fl} CreErT⁺ pancreata exhibited ~90% lower expression of WT *Sec23b* mRNA by qRT-PCR compared to WT pancreata (Figure 1B), with similar decreases in steady state SEC23B protein by Western blot analysis (Figure 1C-D). Since CreErT is expressed only in acinar cell (Ji et al., 2008), some or all of the residual SEC23B expression could be derived from islet and other non-acinar cells. Thus, these data are consistent with high level excision of *Sec23b* in pancreatic acinar cells post-tamoxifen administration. *Sec23a* mRNA and protein levels were not increased in pancreata of mice with acinar cell deletion of *Sec23b* (Figure 1 E-G).

Depletion of *Sec23b* in acinar cells of adult mice results in lower pancreatic weights

One week post-tamoxifen administration, mice were euthanized and pancreata were dissected and weighed. Mice with acinar cell deletion of *Sec23b* (*Sec23b*^{fl/fl} CreErT⁺ or *Sec23b*^{fl/fl} CreErT⁺ mice) exhibited ~40% decrease in pancreatic weight compared to WT control mice (*Sec23b*^{fl/fl} CreErT⁻, *Sec23b*^{+/fl} CreErT⁻, *Sec23b*^{+/+} CreErT⁺, and *Sec23b*^{+/+} CreErT⁻ mice) (p<0.0001), while pancreatic weights of mice with heterozygous acinar cell deletion of *Sec23b* (*Sec23b*^{+/-}

CreErT⁺, *Sec23b*^{+/-} CreErT⁻, and *Sec23b*^{+fl/fl} CreErT⁺ mice) were not significantly different than those of WT mice (p=0.09) (Figure 2A).

The mouse weights before and after tamoxifen administration were indistinguishable between mice with acinar depletion of SEC23B and WT control mice (Figures 2 B-C), suggesting no effect of acinar *Sec23b* deletion on food intake or duodenal pathology.

To determine the baseline CreErT activity in the absence of tamoxifen induction, a cohort of mice (*Sec23b*^{-fl/fl} CreErT⁺, *Sec23b*^{fl/fl} CreErT⁺, and WT controls) was gavaged with corn oil not containing tamoxifen. *Sec23b*^{-fl/fl} CreErT⁺ and *Sec23b*^{fl/fl} CreErT⁺ mice exhibited ~13% lower pancreatic weights compared to WT mice (p=0.03) (Figure 2D), explaining only a portion of the decrease in pancreatic weight observed in *Sec23b*^{-fl/fl} CreErT⁺ and *Sec23b*^{fl/fl} CreErT⁺ mice following tamoxifen administration.

To determine if the pancreatic weight following *Sec23b* acinar cell deletion would drop further with time, a cohort of mice were followed for 2 weeks after administration of tamoxifen. The latter mice exhibited a ~40% decrease in pancreas weight compared to WT control mice (Figure 2 E), which is indistinguishable from the drop observed 1 week after tamoxifen administration.

The lower pancreatic weights in mice with acinar deletion of *Sec23b* is due to cell loss

One week post-tamoxifen administration, total pancreatic DNA, RNA, and protein contents were calculated. Mice with acinar cell deletion of *Sec23b* exhibited an ~43% decrease in pancreatic DNA content (p=0.01, Figure 2F), a ~53% decrease in RNA content (p<0.0001, Figure 2G), and a ~46% decrease in protein content (p<0.0001, Figure 2H) compared to WT mice. The total DNA, RNA, and protein contents of pancreas tissues are decreased proportionately to the decrease in pancreas weights resulting from *Sec23b* deletion in acinar cells, indicating that the decreased pancreas weight can be fully explained by a reduction in cell number, not cell size.

Acinar *Sec23b* deletion results in degeneration of exocrine cells, decreased zymogen granules, and ER alterations

One week following acinar cell-specific deletion of *Sec23b*, histologic evaluation of pancreas tissues demonstrated smaller than normal pancreata with mild to moderate disruption of normal lobular architecture due to multifocal degeneration of exocrine epithelial cells within pancreatic lobules, with shrinkage of lobules and prominence of supporting stroma and periductular fibrosis. Degenerate acinar cells were shrunken with loss of zymogen granules, condensed nuclei and cytoplasmic enhancement of the eosin stain (Figure 3A). Histologic evaluation of pancreas tissues performed 2 weeks after tamoxifen administration revealed comparable findings (Supplemental Figure 1A).

Alteration in acinar morphology following *Sec23b* excision was also assessed by electron microscopy (Figure 4). Seven days following tamoxifen treatment, acinar cell structure in pancreata of WT mice exhibited the expected concentration of zymogen granules surrounding the acinar lumen in the apical pole of the cell and abundant rough ER in basolateral regions (Figure 4A). In contrast, the majority of acinar cells in *Sec23b^{-fl}* CreErT⁺ mice exhibited striking abnormalities, including decreased zymogen granules (Figure 4) and alterations in ER morphology ranging from vesicular ER to markedly expanded cisternae with accumulation of moderate density content or intracisternal granules (Figure 4, B-F). Cells containing vesicular ER often showed ribosomes associated with only portions of the vesicular membrane (Figure 4, F and inset). Many acinar cells showed alteration in their general polarity with granules accumulating in basal regions of the cell, whereas other cells had greatly reduced granule densities. The acinar cell morphology was also assessed 14 days following administration of tamoxifen, demonstrating similar findings observed at the earlier time point (Supplemental Figure 2).

***Sec23b* deletion in acinar cells fails to produce clear manifestations of acute pancreatitis**

One week post tamoxifen administration, random blood glucose and plasma amylase levels were measured. Mice with acinar cell deletion of *Sec23b* exhibited indistinguishable blood glucose (Figure 5A) and plasma amylase levels (Figure 5B) compared to mice heterozygous for *Sec23b* in their acinar cells and to WT controls. In addition, a small number of white blood cells (mostly resident macrophages and lymphocytes) was observed by immunohistochemistry, but much less than that observed in the pancreatitis positive control samples, which contained a significant number of neutrophils in addition to large numbers of other inflammatory cells (Figure 3 B-C and Supplemental Figure 1 B-C). Carboxypeptidase A1 cleavage, which is seen in pancreatitis (Leach et al., 1991), was not observed in pancreas tissues of mice with acinar *Sec23b* deletion (Figure 5C). Other pancreas digestive enzymes were variably affected relative to total protein. Amylase was decreased in total pancreatic cell lysates prepared from mice with acinar deletion of *Sec23b* compared to WT mice (Figure 5D) with a less clear effect on chymotrypsin and trypsin (Figure 5E).

Acinar *Sec23b* deletion results in ER stress and increased apoptosis

To determine whether the ER dilatation observed following acinar *Sec23b* deletion is associated with induction of ER stress and the unfolded protein response (UPR), the expression level of a panel of associated genes was determined by qRT-PCR. Expression for many of these genes was increased following acinar *Sec23b* deletion, with the increase in *Eif2a* and *Grp94*, reaching statistical significance ($p < 0.05$) (Figure 6A).

Following tamoxifen administration, TUNEL assays were also performed on pancreatic tissues harvested from *Sec23b^{-fl}* CreErT⁺ mice and WT controls (Figure 6B, panels a-d). Three days post-tamoxifen administration, the

percentage of TUNEL positive cells in *Sec23b*^{-fl} CreErT⁺ mice (6.08%) was higher than that in WT control mice (0.04%) (Figure 6C). The same pattern was also observed 7-days post-tamoxifen administration (1.62% and 0.11% respectively) (Figure 6C). Consistent with these results, the expression of activated caspase 3 was increased in pancreata of *Sec23b*^{-fl} CreErT⁺ mice compared to WT control mice (Figure 6B, panels e and f).

Discussion

Mice with germline deletion of *Sec23b* die perinatally, exhibiting massive pancreatic degeneration (Tao et al., 2012). Pancreas-specific *Sec23b* deletion in developing mouse embryos recapitulates the phenotype of mice with global SEC23B deficiency (Khoriaty et al., 2016), demonstrating that the defect in the latter mice is intrinsic to the pancreas. It is not clear if this effect is mediated by the loss of the endocrine or exocrine pancreas or the development of intrauterine pancreatitis.

In this report, we evaluated the impact of SEC23B depletion in adult pancreatic acinar cells by generating mice with tamoxifen-inducible acinar cell specific SEC23B deficiency. Tissue was evaluated from 3 days to 2 weeks after tamoxifen. Tamoxifen administration to these adult mice results in pancreatic cell loss, swollen ER with degeneration of exocrine cells, ER stress, and increased pancreatic acinar cell apoptosis but without an effect on viability of the mice. There were small numbers of white blood cells (primarily resident macrophages and lymphocytes) in pancreatic tissues of the latter mice; these infiltrates were minimal in comparison to the moderate inflammatory cell infiltration in the pancreatitis positive control tissues. In addition, the pancreatitis control tissues exhibited a significant number of neutrophils, consistent with a primary inflammatory process in the pancreas. In contrast, the small numbers of macrophages observed in the pancreas of *Sec23b* depleted mice is consistent with a clean-up process secondary to acinar degeneration, rather than an active inflammatory process. Additionally, amylase was not increased in the plasma of mice with acinar depletion of *Sec23b* and carboxypeptidase cleavage was not observed, arguing against frank pancreatitis. Taken together, these data demonstrate that SEC23B is important for maintenance of function of adult murine pancreatic acinar cells. Specifically, the results are consistent with a role for SEC23B in forming the COPII coat, which promotes budding of transport vesicles off the ER initiating passage through the secretory pathway culminating in the production of ZG. Blockage of the early secretory pathway explains the reduction in ZG. Since some granules are still present, the blockage is not complete. Interestingly, different digestive enzymes move through the pathway to the ZG at different rates. Chymotrypsinogen is known to move faster and shows a higher step up in concentration than amylase (Oprins et al., 2001). The slower movement of amylase may be related to the overall fall in tissue amylase compared to chymotrypsinogen, which does not fall in SEC23B deficiency.

In contrast to mice with germline SEC23B deficiency, *Sec23b* deletion in pancreatic acinar cells of adult mice is not lethal (a cohort of mice was followed for ~2-3 weeks post-tamoxifen administration). One possible explanation is that these mice were observed for too short of a time period post-tamoxifen administration to assess for mortality. Alternatively, selection over time against acinar cells with complete *Sec23b* excision could result in enrichment for normal acinar cells with intact *Sec23b*. Another possible explanation is that the small percentage of acinar cells without *Sec23b* excision might be sufficient for survival of these mice. It is also possible that *Sec23b* exerts a unique function during murine embryonic development, which is responsible for the damage in the setting of germline deletion.

Acinar cell death following *Sec23b* deletion could result from accumulation of exocrine pancreatic enzymes in the ER resulting in ER stress and apoptosis. Consistent with this hypothesis, mutations in *PRSS1*, the gene encoding trypsinogen, which result in an increase of its activity, have been associated with pancreatitis (Ferec et al., 1999; Whitcomb et al., 1996a; Whitcomb et al., 1996b). Similarly, mutation in *SPINK1*, which encodes a serine protease with antitrypsin activity, have been shown to be associated with hereditary pancreatitis (Audrezet et al., 2002; Witt et al., 2000). However, these genes are involved in enhancing or inhibiting the activity of trypsin while still in the acinar cell. Deletion of SEC23B inhibits exit from the ER but is not expected to affect trypsin activation and for this reason may not promote pancreatitis in the adult mouse. Recently, variants in procarboxypeptidase A1 in humans were shown to be associated with pancreatitis associated with ER stress but without trypsin activation (Witt et al., 2013). Further work on the type of ER stress induced by *Sec23b* deletion in murine acinar cells is warranted.

Materials and Methods

Mice and PCR genotyping

A *Sec23b* floxed allele (*Sec23b^{fl}*) and a *Sec23b* null allele (*Sec23b⁻*) were generated as previously described (Figure 1A) (Khoriaty et al., 2014). Mice carrying a pancreatic acinar cell specific tamoxifen-inducible Cre-recombinase (CreErT) transgene (a generous gift from C. Logsdon) (Ji et al., 2008), were crossed to *Sec23b^{+/-}* mice to generate *Sec23b^{+/-}* CreErT⁺ mice. CreErT mice express Cre recombinase under the control of the full-length elastase gene promoter resulting in expression of Cre recombinase in nearly 100% of the acinar cells but not in duct or islet cells (Gurda et al., 2010; Ji et al., 2008). Genotyping for the *Sec23b^{fl}*, *Sec23b⁻*, and CreErT alleles was performed as previously described (Ji et al., 2008; Khoriaty et al., 2014). All the mice utilized in this study were either generated on the C57BL/6J background or have been crossed to the latter genetic background for more than 6 generations.

A cohort of wild type mice, were given cerulein (50 ug/kg) every hour for 7 hours to induce pancreatitis as previously described (Sans et al., 2003). These mice, which exhibit increased plasma amylase and pancreatic cell damage, were used as positive control for pancreatitis.

Tamoxifen administration

Tamoxifen (purchased from Sigma) was dissolved in corn oil at 10 mg/ml. Five to six week old mice were administered tamoxifen (3 mg tamoxifen per 40 grams of mouse weight) via daily gavage for 4 days.

Blood glucose and amylase measurement

Blood glucose was measured using the one touch ultra glucometer (LifeScan) or the contour glucometer (Bayer) and plasma amylase was measured using Phadebas reagents (Magle Life Sciences) according to manufacturer's instructions.

DNA, RNA, and protein isolation and measurement

Pancreas tissue samples were weighed and homogenized at 100 mg / 1.5 ml solution of 5mM MgCl₂ + 0.1% Triton X-100, then sonicated. DNA and RNA were measured using the Qubit RNA HS Assay kit (Life Technologies, catalog number Q32852) and Qubit dsDNA HS Assay kit (Life Technologies, catalog number Q32851), respectively, and according to manufacturer's instructions. Protein was measured spectrophotometrically by using Bio-Rad protein assay reagent. Total pancreatic protein, DNA and RNA were then calculated (Crozier et al., 2010; Tashiro et al., 2004).

qRT-PCR

RNA was isolated from pancreas tissues using the RNeasy kit (Qiagen). cDNA synthesis was carried out using the Superscript First-Strand Synthesis System for RT-PCR (Invitrogen) with random primers. Power SYBR Green PCR Master Mix (Applied Biosystems) was used for quantitative RT-PCR using the Applied Biosystems 7900HT Fast real-time PCR System. Each sample was analyzed in triplicate, and *Gapdh* or *Atcb* (β -actin) were used as internal controls. Relative gene expression was determined using the $2^{-\Delta\Delta CT}$ method. Primers used are listed in Supplementary Table 1.

Western blot and antibodies

Total cell lysates were prepared from pancreas tissues, and western blots (film visualization with chemiluminescent detection) were performed as previously described (Khoriaty et al., 2014). Mouse anti-Actin and anti-GAPDH antibodies were obtained from Santa Cruz and Millipore, respectively. Rabbit anti-SEC23B and anti-SEC23A antibodies were generated as previously described (Khoriaty et

al., 2014). Carboxypeptidase A1, Amylase, chymotrypsin, and trypsin antibodies were obtained from R&D Systems (AF2765), Sigma (A8273), Fitzgerald (20C-CR1095R), and Santa Cruz (sc-67388), respectively. Quantitative Western blots (infrared fluorescent detection) were performed and analyzed as previously described (Khoriaty et al., 2016).

Hematoxylin and eosin staining and electron microscopy

Pancreas tissues were collected and fixed in 4% paraformaldehyde for histologic analysis. Tissues were processed, embedded in paraffin, sectioned at 4 μm , and stained with hematoxylin and eosin (H&E). Electron microscopy was performed on pancreas tissues as previously described (Crozier et al., 2009; Hou et al., 2015). In brief, minced pancreas was fixed in a mixture of 2% formaldehyde and 2% glutaraldehyde in phosphate buffered saline, post-fixed in 1% Osmium tetroxide and then dehydrated and embedded in Epon. Ultrathin sections were stained with uranyl acetate and lead citrate and evaluated with a Phillips CM-100 electron microscope.

Immunohistochemistry

Immunohistochemistry was performed as previously described (Khoriaty et al., 2016) with anti-CD45 and anti-F4/80 antibodies purchased from Novus Biologicals (NB100-77417) and Abcam (ab6640), respectively.

TUNEL assay and caspase 3 immunostaining

ApopTag Red In Situ Apoptosis Detection Kit (Chemicon, Millipore) was used to localize red fluorescent TUNEL positive nuclei. Briefly, fresh frozen sections of pancreas were fixed for 10 minutes with a 2:1 mixture of methanol and acetone at -20°C . Sections were treated with the kit reagents as specified by the manufacturer, coverslipped with mounting medium containing fluorescent nuclear stain DAPI (Prolong Gold, Invitrogen), and viewed with a 40X objective of an Olympus BX-51 fluorescence microscope. Five randomly chosen DAPI-stained fields in sections from each animal were photographed, each followed by changing filters to photograph TUNEL fluorescence. DAPI-stained nuclei were counted using the Nuclei Counting program in Meta Morph software (Molecular Devices, Sunnyvale, CA), while TUNEL-positive nuclei were counted manually. The percent of TUNEL positive nuclei was calculated for each field (5 determinations per mouse) and these values were then averaged for each mouse. This experiment was performed by an investigator blinded to the genotypes of the mice from which the pancreas tissues were harvested.

Immunofluorescence localization of caspase-3 (8G10 rabbit monoclonal antibody, Cell Signaling Technology, Danvers, MA and Alexa anti-rabbit 594, Thermo Fisher Scientific Corp., Grand Island, NY) was performed on cryostat sections of pancreas tissue that has been fixed in 4% paraformaldehyde. Immunostaining for caspase-3 was merged with its corresponding Nomarski image to show acinar cell distribution of caspase-3.

Statistical analysis

The Chi-square test was used to determine the statistical significance of the deviation from Mendelian ratios for mouse crosses. The student's t-test was used to calculate the statistical significance of the differences between various parameters among different genotype groups. P-value < 0.05 is considered statistically significant.

Acknowledgments

This work was supported by National Institute of Health Grants R01 HL039693 and P01-HL057346 (DG), K08 HL128794 (RK), and R37-DK041122 (JAW). RK is a recipient of the American Society of Hematology Scholar Award. DG is a Howard Hughes Medical Institute investigator. The authors would like to acknowledge Elizabeth Hughes, Keith Childs, and Thomas Saunders for preparation of gene targeted mice and the Transgenic Animal Model Core of the University of Michigan's Biomedical Research Core Facilities. Core support was provided by the University of Michigan Cancer Center (P30 CA046592), and Peptide Center (P30 DK34933).

References

- Audrezet, M.P., Chen, J.M., Le Marechal, C., Ruzsniowski, P., Robaszekiewicz, M., Raguenes, O., Quere, I., Scotet, V., and Ferec, C. (2002). Determination of the relative contribution of three genes-the cystic fibrosis transmembrane conductance regulator gene, the cationic trypsinogen gene, and the pancreatic secretory trypsin inhibitor gene-to the etiology of idiopathic chronic pancreatitis. *European journal of human genetics : EJHG* *10*, 100-106.
- Barlowe, C., and Helenius, A. (2016). Cargo capture and bulk flow in the early secretory pathway. *Annu. Rev. Cell Dev. Biol.* *32*, 197-222.
- Bianchi, P., Fermo, E., Vercellati, C., Boschetti, C., Barcellini, W., Iurlo, A., Marcello, A.P., Righetti, P.G., and Zanella, A. (2009). Congenital dyserythropoietic anemia type II (CDAII) is caused by mutations in the SEC23B gene. *Hum Mutat* *30*, 1292-1298.
- Bonifacino, J.S., and Glick, B.S. (2004). The mechanisms of vesicle budding and fusion. *Cell* *116*, 153-166.
- Boyadjiev, S.A., Kim, S.D., Hata, A., Haldeman-Englert, C., Zackai, E.H., Naydenov, C., Hamamoto, S., Schekman, R.W., and Kim, J. Cranio-lenticulo-sutural dysplasia associated with defects in collagen secretion. *Clin Genet* *80*, 169-176.
- Crozier, S.J., D'Alecy, L.G., Ernst, S.A., Ginsburg, L.E., and Williams, J.A. (2009). Molecular mechanisms of pancreatic dysfunction induced by protein malnutrition. *Gastroenterology* *137*, 1093-1101, 1101 e1091-1093.
- Crozier, S.J., Sans, M.D., Wang, J.Y., Lentz, S.I., Ernst, S.A., and Williams, J.A. (2010). CCK-independent mTORC1 activation during dietary protein-induced exocrine pancreas growth. *American journal of physiology. Gastrointestinal and liver physiology* *299*, G1154-1163.

Ferec, C., Raguene, O., Salomon, R., Roche, C., Bernard, J.P., Guillot, M., Quere, I., Faure, C., Mercier, B., Audrezet, M.P., *et al.* (1999). Mutations in the cationic trypsinogen gene and evidence for genetic heterogeneity in hereditary pancreatitis. *Journal of medical genetics* 36, 228-232.

Gorelick, F., and Jamieson, J. (2012). Structure-function relationship in the pancreatic acinar cell. In *Physiology of the Gastrointestinal Tract*, L. Johnson, ed. (Academic Press), pp. 1341-1360.

Gurda, G.T., Crozier, S.J., Ji, B., Ernst, S.A., Logsdon, C.D., Rothermel, B.A., and Williams, J.A. (2010). Regulator of calcineurin 1 controls growth plasticity of adult pancreas. *Gastroenterology* 139, 609-619, 619 e601-606.

Hou, Y., Ernst, S.A., Stuenkel, E.L., Lentz, S.I., and Williams, J.A. (2015). Rab27A Is Present in Mouse Pancreatic Acinar Cells and Is Required for Digestive Enzyme Secretion. *PLoS One* 10, e0125596.

Ji, B., Song, J., Tsou, L., Bi, Y., Gaiser, S., Mortensen, R., and Logsdon, C. (2008). Robust acinar cell transgene expression of CreErT via BAC recombineering. *Genesis* 46, 390-395.

Khoriaty, R., Everett, L., Chase, J., Zhu, G., Hoenerhoff, M., McKnight, B., Vasievich, M.P., Zhang, B., Tomberg, K., Williams, J., *et al.* (2016). Pancreatic SEC23B deficiency is sufficient to explain the perinatal lethality of germline SEC23B deficiency in mice. *Scientific reports* 6, 27802.

Khoriaty, R., Vasievich, M.P., and Ginsburg, D. (2012). The COPII pathway and hematologic disease. *Blood* 120, 31-38.

Khoriaty, R., Vasievich, M.P., Jones, M., Everett, L., Chase, J., Tao, J., Siemieniak, D., Zhang, B., Maillard, I., and Ginsburg, D. (2014). Absence of a red blood cell phenotype in mice with hematopoietic deficiency of SEC23B. *Molecular and cellular biology*.

Klumperman, J. (2000). Transport between ER and Golgi. *Curr Opin Cell Biol* 12, 445-449.

Lang, M.R., Lapierre, L.A., Frotscher, M., Goldenring, J.R., and Knapik, E.W. (2006). Secretory COPII coat component Sec23a is essential for craniofacial chondrocyte maturation. *Nat Genet* 38, 1198-1203.

Leach, S.D., Modlin, I.M., Scheele, G.A., and Gorelick, F.S. (1991). Intracellular activation of digestive zymogens in rat pancreatic acini. Stimulation by high doses of cholecystokinin. *J Clin Invest* 87, 362-366.

Martinez-Menarguez, J.A., Geuze, H.J., Slot, J.W., and Klumperman, J. (1999). Vesicular tubular clusters between the ER and Golgi mediate concentration of soluble secretory proteins by exclusion from COPI-coated vesicles. *Cell* 98, 81-90.

Oprins, A., Rabouille, C., Posthuma, G., Klumperman, J., Geuze, H.J., and Slot, J.W. (2001). The ER to Golgi interface is the major concentration site of secretory proteins in the exocrine pancreatic cell. *Traffic* 2, 831-838.

Sans, M.D., DiMugno, M.J., D'Alecy, L.G., and Williams, J.A. (2003). Caerulein-induced acute pancreatitis inhibits protein synthesis through effects on eIF2B and eIF4F. *American journal of physiology. Gastrointestinal and liver physiology* 285, G517-528.

Schwarz, K., Iolascon, A., Verissimo, F., Trede, N.S., Horsley, W., Chen, W., Paw, B.H., Hopfner, K.P., Holzmann, K., Russo, R., *et al.* (2009). Mutations affecting the secretory COPII coat component SEC23B cause congenital dyserythropoietic anemia type II. *Nat Genet* 41, 936-940.

Tao, J., Zhu, M., Wang, H., Afelik, S., Vasievich, M.P., Chen, X.W., Zhu, G., Jensen, J., Ginsburg, D., and Zhang, B. (2012). SEC23B is required for the maintenance of murine professional secretory tissues. *Proc Natl Acad Sci U S A* 109, E2001-2009.

Tashiro, M., Samuelson, L.C., Liddle, R.A., and Williams, J.A. (2004). Calcineurin mediates pancreatic growth in protease inhibitor-treated mice. *American journal of physiology. Gastrointestinal and liver physiology* 286, G784-790.

Whitcomb, D.C., Gorry, M.C., Preston, R.A., Furey, W., Sossenheimer, M.J., Ulrich, C.D., Martin, S.P., Gates, L.K., Jr., Amann, S.T., Toskes, P.P., *et al.* (1996a). Hereditary pancreatitis is caused by a mutation in the cationic trypsinogen gene. *Nat Genet* 14, 141-145.

Whitcomb, D.C., Preston, R.A., Aston, C.E., Sossenheimer, M.J., Barua, P.S., Zhang, Y., Wong-Chong, A., White, G.J., Wood, P.G., Gates, L.K., Jr., *et al.* (1996b). A gene for hereditary pancreatitis maps to chromosome 7q35. *Gastroenterology* 110, 1975-1980.

Witt, H., Beer, S., Rosendahl, J., Chen, J.M., Chandak, G.R., Masamune, A., Bence, M., Szmola, R., Oracz, G., Macek, M., *et al.* (2013). Variants in CPA1 are strongly associated with early onset chronic pancreatitis. *Nature Genetics* 45, 1216-U1359.

Witt, H., Luck, W., Hennies, H.C., Classen, M., Kage, A., Lass, U., Landt, O., and Becker, M. (2000). Mutations in the gene encoding the serine protease inhibitor, Kazal type 1 are associated with chronic pancreatitis. *Nat Genet* 25, 213-216.

Zanetti, G., Pahuja, K.B., Studer, S., Shim, S., and Schekman, R. (2012). COPII and the regulation of protein sorting in mammals. *Nat Cell Biol* 14, 20-28.

Zhu, M., Tao, J., Vasievich, M.P., Wei, W., Zhu, G., Khoriaty, R.N., and Zhang, B. (2015). Neural tube opening and abnormal extraembryonic membrane development in SEC23A deficient mice. *Scientific reports* 5, 15471.

Figure legends

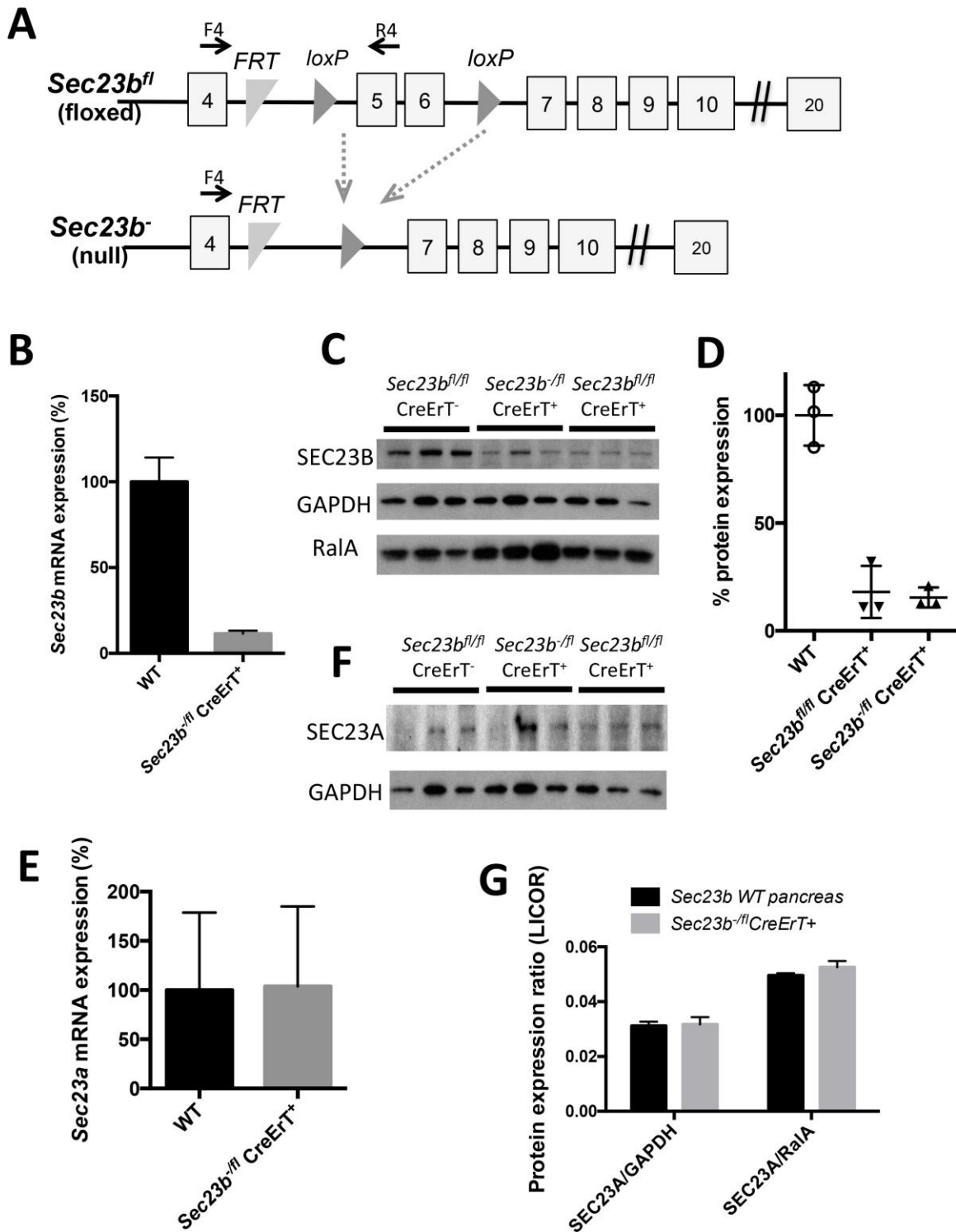


Figure 1. *Sec23b* inactivation in pancreatic acinar cells. (A) *Sec23b* alleles (not drawn to scale (Khoriaty et al., 2014)). Each square indicates an exon and horizontal lines between exons indicate introns. F4 and R4 are primers used for assessing efficiency of cre-mediated excision. (B) *Sec23b* excision determined by qPCR (n = 3 for each genotype) and (C) western blot on pancreas tissues 7

days post-administration of tamoxifen. (D) Quantification of the SEC23B band intensities in panel C relative to the average of GAPDH and RalA was performed using ImageJ. (E-F) Quantitation of *Sec23a* expression by (E) qPCR (n = 3 controls and 4 *Sec23b*^{-fl} CreErT⁺ mice), (F) chemiluminescent western blot detection, and (G) quantitative western blot (infrared fluorescent detection) in pancreas tissues 7 days post-administration of tamoxifen (n = 3 mice per genotype).

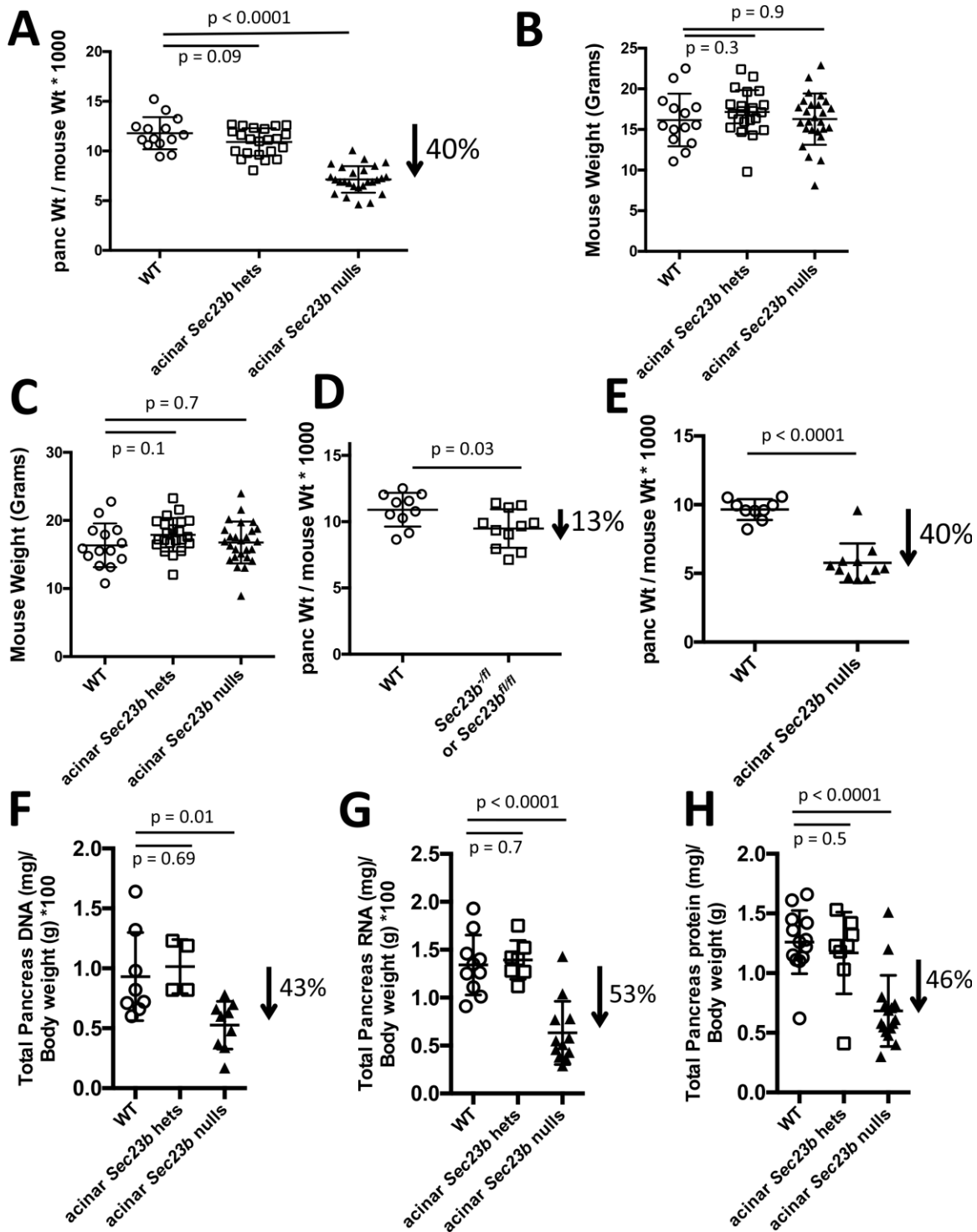


Figure 2. *Sec23b* deletion in acinar cells results in decreased pancreatic weight from cell loss. (A) Ratios of pancreas to total body weight 7 days after administration of tamoxifen indicate substantial loss of pancreas weight resulting from inactivation of *Sec23b* in pancreas acinar cells. (B) Mice weights before and (C) one week after tamoxifen administration indicates no loss of total body weight with acinar deletion of *Sec23b*. (D) Ratios of pancreas to total body weight 7

days after administration of corn oil demonstrate that only a small portion of the pancreatic weight loss is explained by basal CreErT activity in the absence of tamoxifen induction. (E) A cohort of mice were evaluated 14 days after tamoxifen administration, demonstrating no continued drop in pancreatic weight compared to evaluation performed 7 days following tamoxifen in panel A. The loss of pancreatic weight is associated with a comparable degree of decrease in pancreas (F) DNA, (F) RNA, and (H) total protein, consistent with cell loss. Each data point represents one mouse.

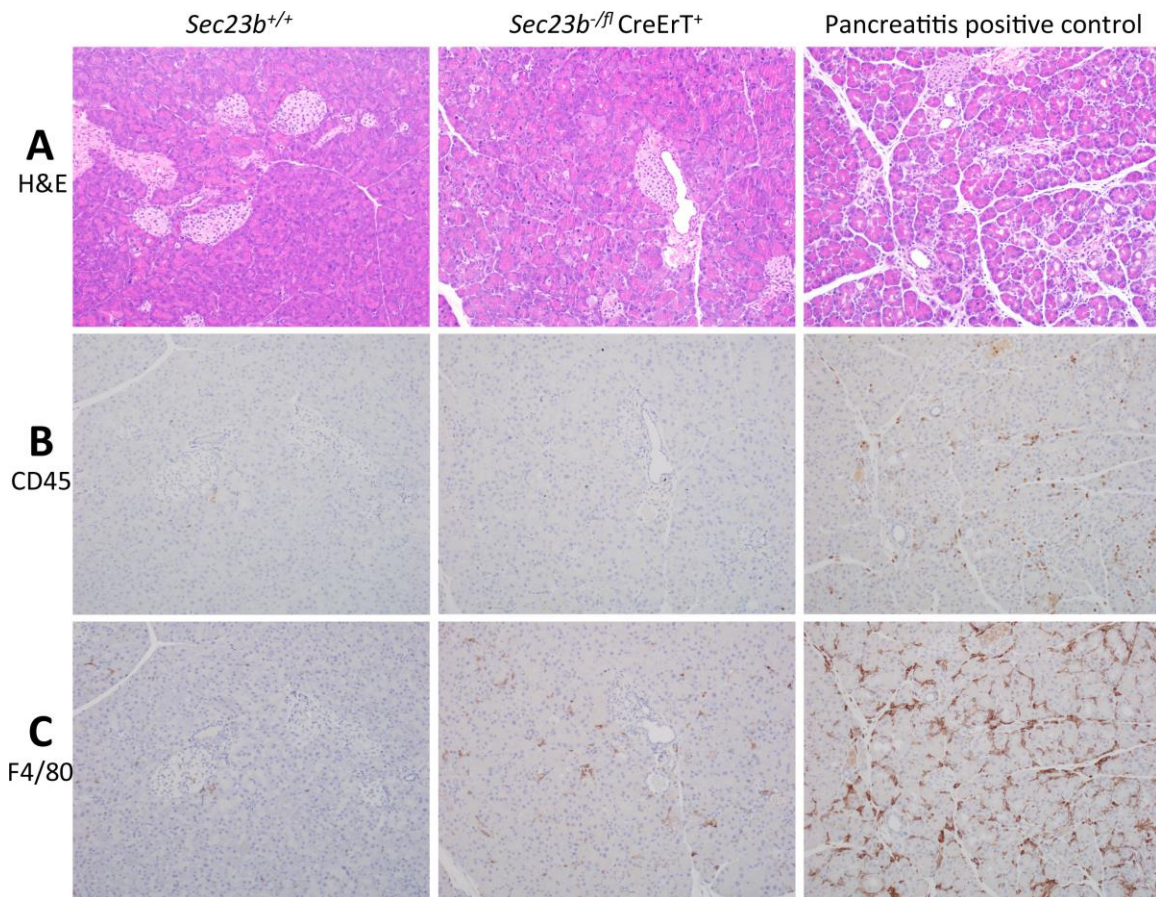


Figure 3. Histologic evaluation of pancreas tissues 7 days following deletion of acinar *Sec23b*. The evaluation was performed by an investigator blinded to the genotypes of the mice from which the tissues were derived (four mice of each genotype were evaluated). (A) Seven days following acinar *Sec23b* deletion, evaluation of pancreas tissues by hematoxylin and eosin stains demonstrated overall loss of parenchymal size and lobular atrophy due to degeneration of acinar epithelial cells characterized by cellular shrinkage, cytoplasmic loss with loss of zymogen granules, enhancement of the eosin stain, and nuclear pyknosis (middle panel) compared to WT controls (left panel). Positive control for pancreatitis 1 day after cerulean treatment is shown in the right panel. (B) Immunohistochemistry for CD45 and (C) for F4/80 demonstrates a small number of white blood cells (mostly macrophages) infiltrating pancreas tissues of mice

with acinar *Sec23b* deletion, compared to to mice with cerulean-induced pancreatitis (positive control).

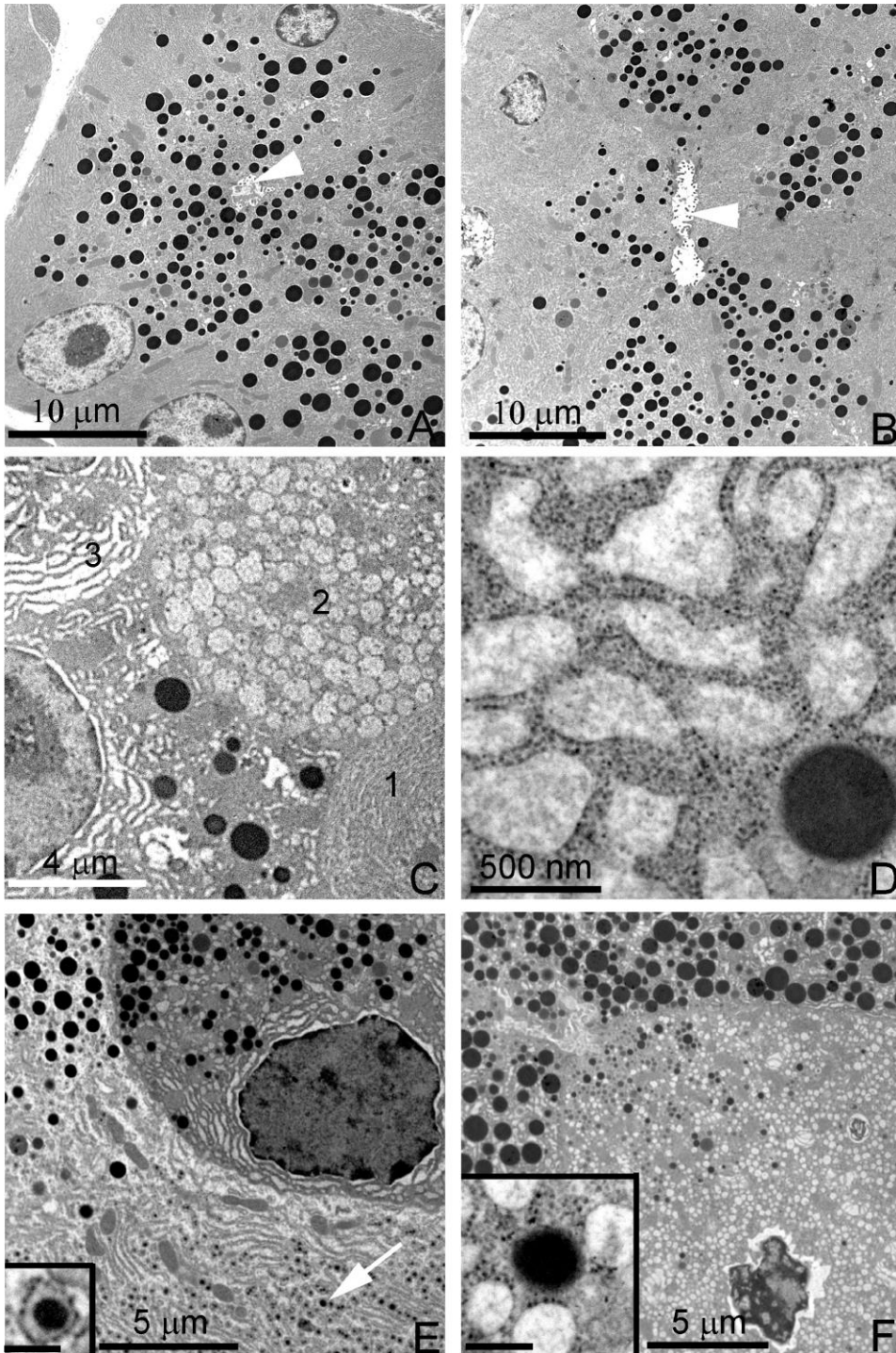


Figure 4. Electron microscopy of pancreas tissues 7 days following deletion of acinar *Sec23b*. Evaluation of pancreas tissues by electron microscopy demonstrates normal acinar morphology in WT control mice with numerous granules adjacent to the lumen (arrowhead) and basal rough ER cisternae (panel

A). Pancreas tissues with acinar deletion of *Sec23b* exhibited variably decreased zymogen granules (panel B; arrowhead denotes ER lumen) as well as multiple alterations, including vesicular or expanded rough ER (cell 2 and 3 panel C, in contrast to normal cell morphology seen in cell 1 panel C), expanded rough ER cisternae with amorphous content (panels C and D), small intracisternal granules (arrow and higher magnification inset, panel E), crenulated nucleus and vesicular rough ER (panel F), with amorphous content and partial studding with ribosomes (panel F and inset). Scale bars are indicated in the figure panels. Scale bars in insets of panels E and F are 250 nm. Three mice of each genotype were evaluated.

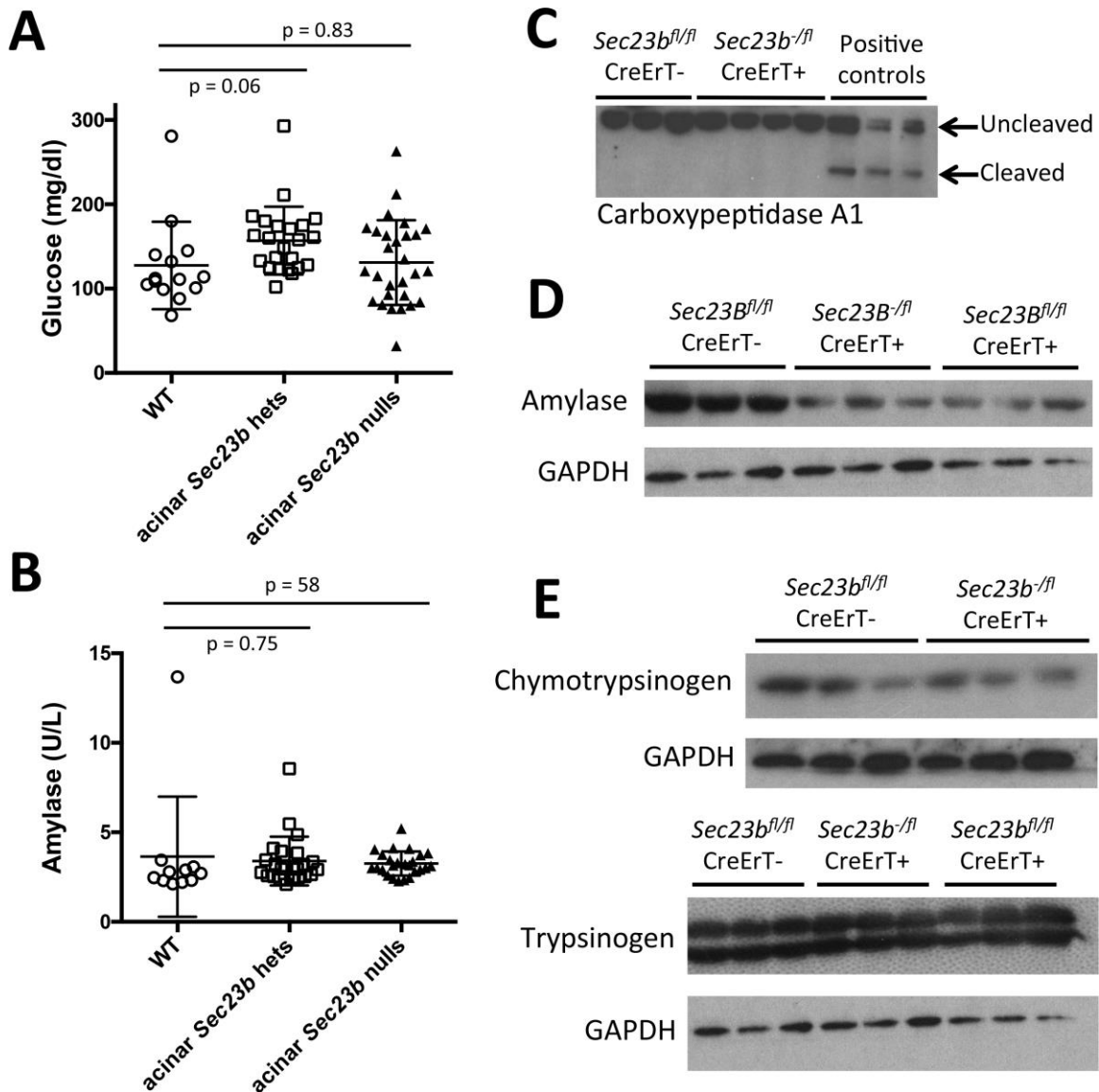


Figure 5. Deletion of *Sec23b* in mouse acinar cells does not affect plasma glucose or amylase but results in decreased pancreatic amylase in total pancreas cell lysates. (A) *Sec23b* deletion in acinar cells does not result in increased plasma glucose or (B) increased plasma amylase (each data point

represents one mouse). (C) Carboxypeptidase cleavage observed in pancreas tissues of mice given cerulein to induce pancreatitis was not observed in pancreas tissues of mice with acinar *Sec23b* inactivation. (D) *Sec23b* deletion in pancreas acinar cells results in decreased pancreatic amylase in total pancreas cell lysates, (E) with a less clear effect on chymotrypsin and trypsin.

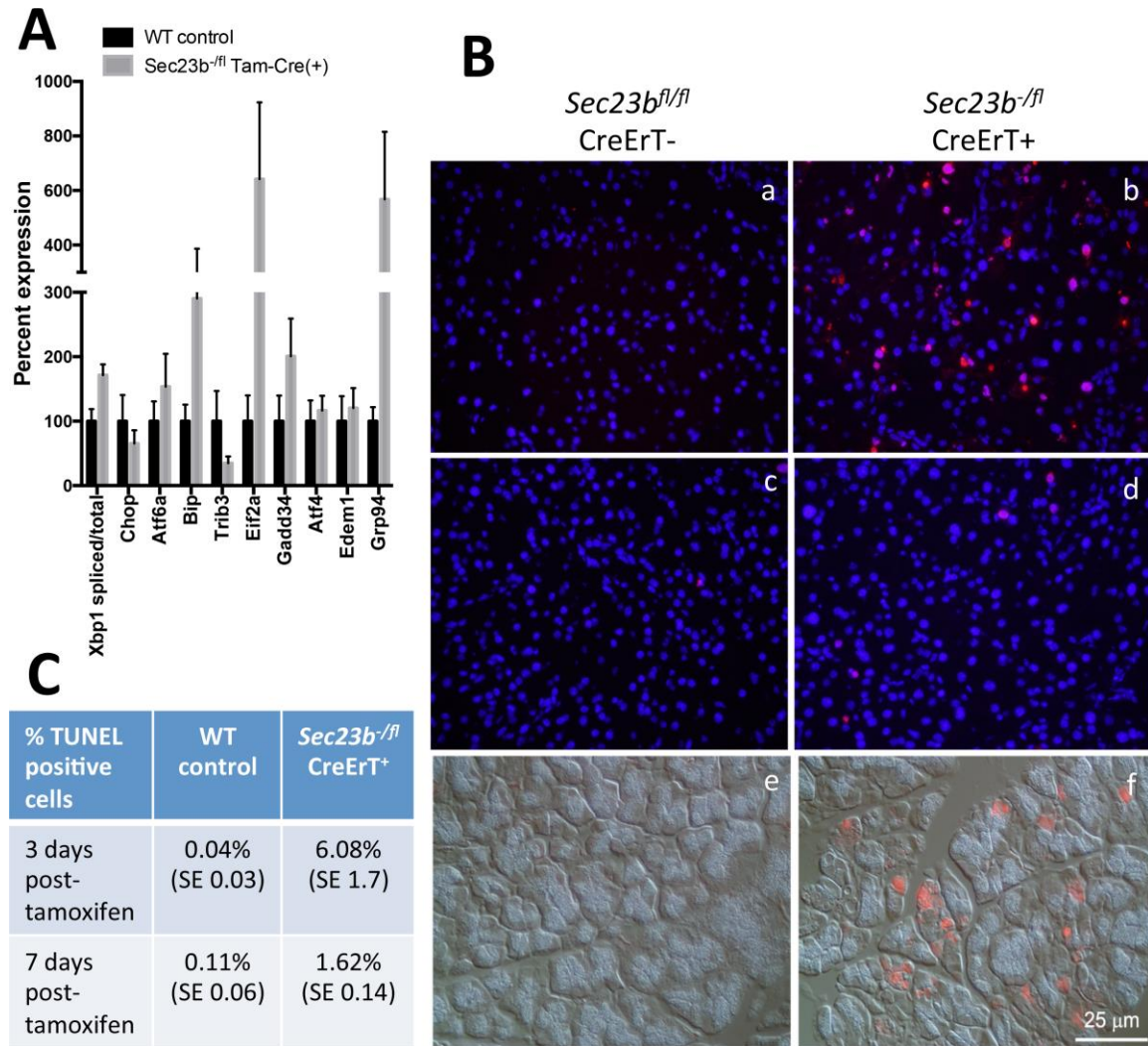


Figure 6. Expression of UPR genes and TUNEL assay in pancreas tissues following acinar *Sec23b* deletion. (A) Real time RT-PCR expression of select UPR genes was performed on pancreas tissues harvested one week following administration of tamoxifen, with levels normalized to β -actin. Data are represented by mean \pm standard error of the mean. Asterisks indicate statistically significant difference between WT and *Sec23b*^{-/-} CreErT(+) samples. Six mice from each genotype were evaluated. (B) TUNEL assays overlaid on DAPI were performed 3 days (panels a,b) and 7 days (panels c,d) post-administration of tamoxifen. *Sec23b*^{-/-} CreErT⁺ mice exhibit increased apoptosis at both time points. Immunostaining for active caspase 3 demonstrates increased expression in mice with acinar deletion of *Sec23b* (panel f) compared to WT mice (panel e) on Nomarski image. (C) The average percentage of TUNEL positive cells

is shown (3-4 mice were evaluated per condition, and ~2,000-2,500 cells were counted per sample). The evaluation was performed by an investigator blinded to the genotypes of the mice from which the tissues were derived. SE indicate the standard error of the mean.

Table 1. Results of *Sec23b*^{+/-}CreErT(+) x *Sec23b*^{+/*fl*} matings to generate mice with tamoxifen inducible acinar cell specific deletion of *Sec23b*.

A. Genotypes:	<i>Sec23b</i>^{+/+} CreErT(+)	<i>Sec23b</i>^{+/+} CreErT(-)	<i>Sec23b</i>^{+/<i>fl</i>} CreErT(+)	<i>Sec23b</i>^{+/<i>fl</i>} CreErT(-)	<i>Sec23b</i>^{+/-} CreErT(+)	<i>Sec23b</i>^{+/-} CreErT(-)	<i>Sec23b</i>^{-/<i>fl</i>} CreErT(+)	<i>Sec23b</i>^{-/<i>fl</i>} CreErT(-)	p-value*
Expected ratios	12.5%	12.5%	12.5%	12.5%	12.5%	12.5%	12.5%	12.5%	
Observed at weaning % (n=174)	9% (16)	13% (23)	14% (24)	14% (24)	13% (22)	13% (23)	11% (19)	13% (23)	>0.8

* p-value calculated for *Sec23b*^{-/*fl*}CreErT(+) mice versus all other genotypes.